

**Polymer translocation: Effects of confinement**

Manish Dwivedi, Sumitra Rudra, and Sanjay Kumar

*Department of Physics, Banaras Hindu University, Varanasi 221005, India*

(Received 26 June 2023; accepted 24 January 2024; published 27 February 2024)

We investigate the influence of varying confinement on the dynamics of polymer translocation through a cone-shaped channel. For this, a linear polymer chain is modeled using self-avoiding walks on a square lattice. The *cis* side of a cone-shaped channel has a finite volume, while the *trans* side has a semi-infinite space. The confining environment is varied either by changing the position of the back wall while keeping the apex angle fixed or altering the apex angle while keeping the position of the back wall fixed. In both cases, the effective space  $\phi$ , which represents the number of monomers in a chain relative to the total number of accessible sites within the cone, is reduced due to the imposed confinement. Consequently, the translocation dynamics are affected. We analyze the entropy of the confined system as a function of  $\phi$ , which exhibits nonmonotonic behavior. We also calculate the free energy associated with the confinement as a function of a virtual coordinate for different positions of the back wall (base of the cone) along the conical axis for various apex angles. Employing the Fokker-Planck equation, we calculate the translocation time as a function of  $\phi$  for different solvent conditions across the channel. Our findings indicate that the translocation time decreases as  $\phi$  increases, but it eventually reaches a saturation point at a certain value of  $\phi$ . Moreover, we highlight the possibility of controlling the translocation dynamics by manipulating the solvent quality across the channel. Furthermore, our investigation delves into the intricacies of polymer translocation through a cone-shaped channel, considering both repulsive and neutral interactions with the channel wall. This exploration unveils nuanced dynamics and sheds light on the factors that significantly impact translocation within confined channels.

DOI: [10.1103/PhysRevE.109.024412](https://doi.org/10.1103/PhysRevE.109.024412)**I. INTRODUCTION**

The translocation of biopolymers through a pore is a fundamental step in many cellular processes, e.g., passage of DNA and RNA through nuclear pores [1], protein transport through membrane channels [2], packaging of genome in bacteriophages, ejection of virus from capsid [3–5], etc. Apart from its biological relevance, interest has also been fueled by its biotechnological applications such as gene therapy, drug delivery, DNA sequencing [6,7], etc. In fact, recent studies have revealed that polymer translocation through pores is a complex process and is governed by the combined effects of various factors, such as the nature of the pore-polymer interaction [8–10], the geometry of the pore [11,12], external driving forces [13], salt concentration [14,15] across the pore, etc. A detailed understanding of the effect of various system parameters on the translocation process is a prerequisite to understand the transport dynamics of the translocating molecule.

For the unforced translocation, the mean passage time  $\tau$  scales as  $N^\alpha$  with  $\alpha = 1 + 2\nu$ , where  $\nu$  is the Flory exponent. However, recent studies suggest that the value of the scaling exponent  $\alpha$  depends on the pore size, apex angle, quality of solvents [16–19], etc. A significant amount of work have been carried out recently to understand the role of the driving force on the translocation. In the case of driven translocation, there exist several possibilities: the driving force could be in the form of chaperon binding [20–22], confinement [23–25], crowders [11,26,27], or an external field [13]. In the case of charged polymers, e.g., DNA, the translocation is driven by an electric field acting across the channel. Kasianowicz *et al.* [6]

studied the translocation of single molecules by measurement of the ionic current passing through pores. The potential difference across the pore drives the ionic current, which also drives charged biopolymers through the pore. The amount of the variation in the ionic current has been used to extract the information about the sequence and length of DNA.

Confinement arising due to the geometry of the pore interface [e.g., Mycobacterium smegmatis porin A (MspA), HIV-1 capsid] also drives the translocation [28]. The geometry of the pore looks similar to a cone-shaped channel (Fig. 1), where the driving force may be due to the different solvents across the pore or entropy gradient because of the shape of the channel [29,30]. The polymer translocation through the cone-shaped channel has been studied experimentally [31–33] and theoretically in recent years. The focus was to obtain scaling associated with translocation [23,25,34–36]. On the other hand, a theoretical understanding of the equilibrium properties of a polymer inside the cone has been achieved through the conformal invariance technique and the exact-enumeration technique followed by the series analysis [37] to calculate various exponents. Using an exact-enumeration technique followed by the Langevin dynamics simulations, Kumar *et al.* [38] showed that the confinement leads to the nonmonotonic behavior in the  $\theta$  temperature, where a polymer chain acquires the globule state from the coil state. Interestingly, by varying the apex angle  $\alpha$ , they showed that the  $\theta$  temperature can be shifted.

In this study, we comprehensively explore polymer translocation dynamics with a focus on the influence of the confining environment. What distinguishes our research are

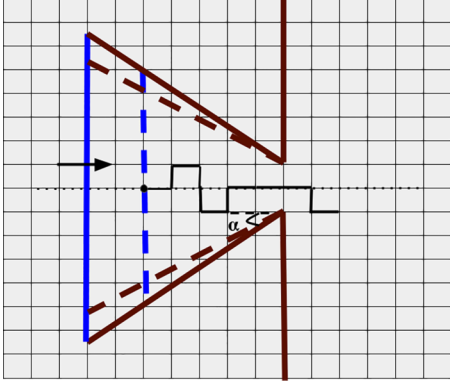


FIG. 1. Schematic representation of a polymer threading through a conical channel (pore) on a square lattice. The impenetrable rigid side walls are depicted as thick brown walls, while the impenetrable rigid back wall is shown as a thick blue line. The conical channel separates the *cis* and *trans* sides, with infinitely extended rigid walls. The confinement within the channel can be adjusted either by changing the position of the back wall, indicated by the dashed blue line, or by varying the angle of the cone, represented by the dashed brown line. The polymer within the channel undergoes a random walk, starting from various positions on the principal axis, denoted by the dotted lines.

three pivotal elements. First, our model realistically features a finite volume on the *cis* side and semi-infinite space on the *trans* side, closely mirroring real-world systems. Second, our model allows for dynamic adjustments in the apex angle and the position of the back wall, potentially inducing shifts in the polymer's center of mass due to changes in geometry. Third, we delve into the entropy variation concerning the back wall position and the apex angle, unveiling the free energy profile of the system and offering insights into the thermodynamics of polymer translocation. Finally, we employ the Fokker-Planck equation to calculate the translocation time as a function of the back-wall position and the effective space available to the polymer. These aspects of our research not only deepen our understanding of polymer translocation, but also illuminate the relatively uncharted territory of confining environment effects on this dynamic process, highlighting the relatively unexplored areas that demand attention within this field. The outline of the paper is as follows.

In Sec. II, we provide a brief overview of the model and detail the techniques employed. Section III focuses on calculating the system's entropy as a function of  $\phi$  and the free energy. Since the exact information of the density of states is known, we employ the Fokker-Planck equation to calculate the time required to cross the channel and termed it the translocation time ( $\tau$ ). In Sec. IV, we investigate the impact of both repulsive and neutral interactions with the channel wall, revealing nuanced dynamics that significantly influence translocation within confined channels. The paper ends with a brief discussion and future perspective of the present study in Sec. V.

## II. MODEL AND METHOD

We investigate a self-avoiding walk model of a linear polymer chain on a square lattice, which is confined in a

cone-shaped channel. The cone-shaped channel consists of two perfectly reflecting hard walls inclined at an apex angle  $\alpha$  (Fig. 1). Only a single monomer is allowed to pass through the opening of the channel, preventing the formation of a fork or hairpin at the channel. To explore the process of translocation resulting from reduced entropy due to the closed cone-shaped channel, we employ an exact-enumeration technique. This technique systematically generates all possible conformations of the polymer and examines whether the polymer resides in the *cis* side (within the channel) or *trans* side (outside the channel) or in a state of threading (from *cis* side to *trans* side). The inherent fourfold symmetry of the square lattice naturally produces angles that are multiples of  $\pi/4$ , such as  $\pi/4$  and  $\pi/2$ . To explore angles beyond these specific multiples, we use an innovative technique outlined in Ref. [39]. Specifically, we consider  $n_x$  bonds along the  $\pm x$  direction, followed by  $+n_y$  bonds in the  $y$  direction. Distinguishing our study from the previous study [39], where the *cis* and *trans* sides were characterized by semi-infinite space, the model developed here represents a significant departure reflecting a fundamental shift towards a more realistic representation of real-world systems. The presence of a perfectly reflecting hard back wall in the conical channel (Fig. 1) alters the translocation dynamics. This marked departure from the conventional semi-infinite space assumption may impact our understanding of polymer translocation within confined environments. The position of the back wall can be placed at different positions of the principal axis (say  $X = -18, -17, \dots$ ) away from the origin. Moreover, the *trans* side is demarcated by a reflecting vertical (perpendicular to the principal axis) hard with a opening of the channel (Fig. 1). It is worth emphasizing that alterations to the apex angle or the back wall's position lead to changes in the available space within the *cis* side. However, in stark contrast, the available space at the *trans* side remains constant and unaffected by variations in the confining environment.

We attached one end of a self-avoiding walk (SAW) at the middle of the back wall, positioned at a distance  $-X$  away from the opening of the channel, and generated all possible conformations of  $N = 28$  steps walk with imposed boundary conditions. We systematically varied the position of the back wall ( $X = -18$  to  $X = -1$ ), and evaluated the partition function as a sum over all possible conformations for different apex angles,

$$Z_X = C_N z^N, \quad (1)$$

where  $C_N$  is the total number of all possible conformations of a polymer chain whose one end is attached on the back wall (Fig. 1), and  $z$  is the fugacity of each step of the walk. For large  $N$ ,  $C_N \sim \mu^N N^{\gamma'-1}$  [40,41]. Here,  $\mu$  is the connectivity constant of the lattice and  $\gamma'$  is the critical exponent associated with the SAW confined in a cone with the apex angle  $\alpha$ . It is important to note that the techniques previously developed and successfully applied in Ref. [39] have established their efficacy in reproducing earlier findings. Building upon this well-established foundation, we have extended these techniques to a more realistic model. This extension allows us to understand translocation in scenarios characterized by diverse geometric considerations and confinement factors.

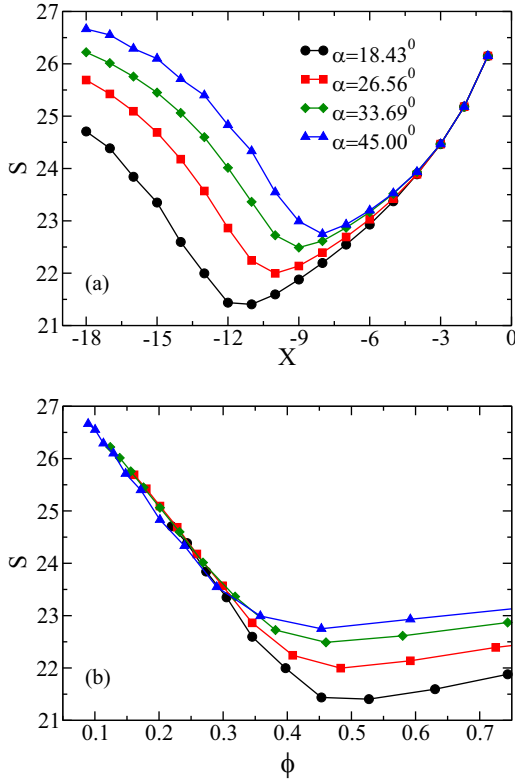


FIG. 2. Figures show a nonmonotonic variation of entropy  $S$  as a function of (a) back-wall position  $X$  and (b) effective space  $\phi$  for different apex angles  $\alpha$ . A nice collapse of data on a single line up to a certain value of  $\phi$  is apparent from the plot.

### III. RESULTS

#### A. Entropy in good solvent

While calculating entropy exactly remains a formidable challenge in most of the theoretical studies, the exact-enumeration technique offers a distinct advantage. With exact knowledge of the density of states, one can compute entropy by exhaustively enumerating all possible configurations within a given system’s complexity. For instance, in the context of polymer translocation, the exact-enumeration method systematically generates all polymer conformations within the *cis* and *trans* side of the cone-shaped channel, providing an exact measure of configurational entropy. This approach serves as a powerful tool for understanding complex systems where analytical solutions are elusive, offering insights into the fine-grained thermodynamics that govern translocation behavior. The entropy of the system is calculated as

$$S = k_B \ln Z_X, \tag{2}$$

where  $k_B$  is the Boltzmann constant.

From here onwards, we work in the reduced energy system by setting  $k_B = 1$ . Since there is no external force on the monomer other than the confinement (due to the back-wall and conical shape of the channel), a polymer comes out from the channel as a result of the entropy difference across the channel. Using Eq. (2), we calculate entropy associated with a polymer chain confined in the conical channel. In Fig. 2, we show the variation of entropy as a function of the position

of the back wall for various apex angles. As the back wall approaches the channel, the entropy of the system decreases. This decline is attributed to the reduction in the number of configurations available to a finite-size polymer within the cone. However, beyond a certain position, we observe a reversal, with entropy increasing once more. This may be attributed to the fact that a part of the chain moves towards the *trans* side, which has more configurational space, and as a result there is an increase in the entropy. To emphasize this behavior, we also plot entropy as a function of the effective space  $\phi$ , representing the fraction of accessible sites within the cone. Remarkably, we observe a collapse of entropy onto a single curve, particularly evident up to a fraction  $\phi \approx 0.3$ , as shown in Fig. 2(b).

#### B. Free energy profile

A comprehensive understanding of the translocation process relies on a complete description of the associated free energy within different regions of the channel. In Ref. [39], we studied the free energy as a function of polymer-pore interaction. However, to unravel the intricate interplay between entropic confinement (arising from the back-wall position or apex angle) and translocation dynamics, we introduce variations in solvent conditions, encompassing both good and poor solvents, across the channel. These varying solvent conditions lead to distinct polymer chain states, from swollen coils in good solvents to collapsed globules in poor solvents. To investigate polymer translocation in these diverse solvents, it is imperative to analyze the time required for each stage of the process, spanning from initiation to completion. Consequently, we divide the translocation into three pivotal stages, each holding unique significance. The initial stage involves the time taken to reach the channel, the second stage is dedicated to the threading process, and the third stage marks the full translocation to the *trans* side.

Throughout these stages, the free energy is associated with a “virtual coordinate” denoted as  $X_V$ , which ranges from  $-X$  to  $2L$ , where  $L = N$ . In stage 1, when the back wall remains fixed at a specific position  $X$  on the principal axis,  $X_V$  corresponds to the physical distance  $x$  from the channel at origin. Here, one end of the polymer is anchored at various  $x$  positions on the principal axis, while the other end is free to be anywhere in the *cis* side of the channel. During this stage,  $X_V$  assumes values within the bounds of the actual coordinates,  $-X \leq X_V < 0$ .

In stage 2, the polymer commences its translocation from the *cis* side to the *trans* side, marking the threading stage. Here,  $X_V = m$  represents the number of monomers that have successfully translocated to the *trans* side, while  $((N + 1) - m - 1)$  monomers remain within the *cis* side of the channel, in addition to a monomer residing at the channel. The final stage 3 manifests as  $X_V$  ranging from  $L + 1$  to  $2L$ , signifying that the polymer has fully emerged from the channel and now exists entirely on the *trans* side. Analogous to stage 1, here  $X_V = L + |x|$ , where  $x$  denotes the physical distance of the polymer’s anchored end on the *trans* side. It is worth noting that while distances from the origin are denoted by  $x$  along the real axis, the free energy is expressed here as a function of the “virtual coordinate”  $X_V$ . The relation between these two

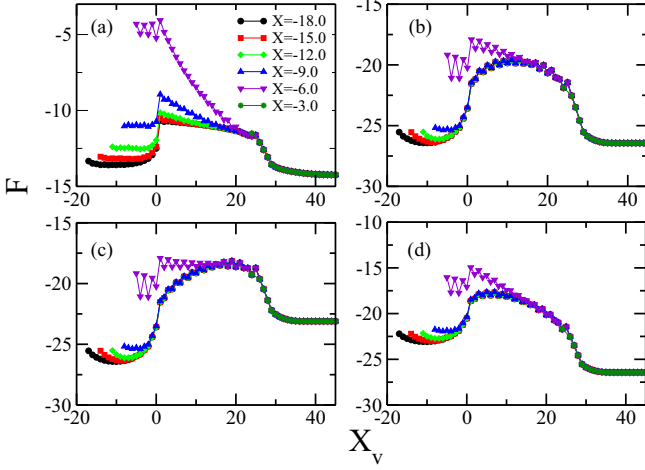


FIG. 3. Free energy as a function of the virtual coordinate  $X_V$  (in the case of apex angle  $\alpha = 45^\circ$ ) for various solvent conditions: (a) good solvent on both the *cis* side and *trans* side ( $\epsilon_c = 0.0 = \epsilon_t$ ), (b) poor solvent on both the *cis* side and *trans* side ( $\epsilon_c = -1.0 = \epsilon_t$ ), (c) the solvent on the *cis* side ( $\epsilon_c = -1.0$ ) is poorer compared to the *trans* side ( $\epsilon_t = -0.8$ ), and (d) the solvent on the *trans* side is poorer compared to the *cis* side ( $\epsilon_c = -0.8$ ,  $\epsilon_t = -1.0$ ).

coordinates is given by [42]

$$X_V = \begin{cases} -|x_i|, & x_i = \dots, -X, \dots, -2, -1 & \text{Stage1} \\ m = i, & i = 0, 1, 2, 3, \dots, L & \text{Stage2} \\ |L + x_i|, & x_i = 1, 2, \dots, L, \dots & \text{Stage3} \end{cases} \quad (3)$$

The partition function, summed over all walks on a square lattice for a virtual coordinate  $X_V$  with a fixed back-wall position  $X$ , is given by the following equation:

$$Z_X(X_V) = \sum_{N_c, N_t} C^{X_V}(N_c, N_t) u^{N_c} v^{N_t}, \quad (4)$$

where  $C^{X_V}(N_c, N_t)$  is the number of conformations of respective stages as defined by Eq. (3).  $N_c$  and  $N_t$  are the number of nearest-neighbor contacts of the *cis* and *trans* sides, respectively.  $u = \exp(-\beta\epsilon_c)$  and  $v = \exp(-\beta\epsilon_t)$  are the Boltzmann weights of nearest-neighbor interactions  $\epsilon_c$  (*cis* side) and  $\epsilon_t$  (*trans* side), respectively. The free energy of the different stages can be obtained from the following equation:

$$F(X_V) = -T \ln Z_X(X_V). \quad (5)$$

The temperature  $T$  is set to 0.5. First, we consider a situation where both *cis* and *trans* sides have a good solvent, i.e.,  $\epsilon_c = \epsilon_t = 0$ . In a good solvent, the polymer adopts a coil-like conformation on both sides of the cone. In Fig. 3(a), we have shown the free energy as a function of virtual coordinate  $X_V$  for different wall positions  $X$ . It is evident from the plots that when one end of the polymer is anchored at a distance far from the opening of the channel, the number of conformations of a polymer remains close to its bulk value and the confinement by the cone-shaped channel does not affect the free energy up to a certain value of  $X_V$ . However, when the anchored site shifts towards the opening of the channel, the polymer conformations get constrained by the cone and, as a result, its configurational properties change relative to its bulk behavior.

Consequently, one observes a change in the free energy at the vicinity of the opening of the channel. Once the threading process starts, the number of conformations of polymer at the *trans* side increases and one observes a gradual decrease in the free energy, followed by a sharp fall, indicating that the entire polymer is translocated from the *cis* side to the *trans* side. As the anchored end of a polymer moves away from the channel, the polymer does not experience any confinement and thus approaches its bulk behavior.

In the presence of a poor solvent on either side of the channel [Fig. 3(b)], we observe a slight reduction in the free energy as the anchored end of a polymer chain approaches the opening of the channel. This results due to an increase in the number of nearest-neighbor contacts because of the confinement imposed by the channel. However, as the anchored site moves closer to the opening of the channel, the number of accessible conformations decreases, leading to an overall increase in the free energy. In contrast to the case of a good solvent, here, during threading, the free energy remains nearly constant. One of the interesting observations is that the free energy almost remains the same for the different wall positions. This behavior can be attributed to the polymer adopting a globule state on both sides, resulting in a sustained level of free energy. Consequently, when a monomer from the globule state on the *cis* side translocates to the *trans* side, it reintegrates into the globule state, thereby maintaining a constant free energy. Similar to the case with a good solvent, in the final stage there is a sharp decrease in the free energy as the polymer assumes its bulk configuration. However, the magnitude of the free energy differs considerably compared to the good solvent.

So far, we have focused on discussing the solvent quality remaining consistent across the channel. It would be interesting to observe how the free energy profile changes when the solvent quality differs across the channel. To investigate the impact of different solvents, we consider two situations: (i) the solvent quality of the *cis* side is relatively poorer compared to the *trans* side ( $\epsilon_c < \epsilon_t$ ), and (ii) the solvent quality on the *trans* side is relatively poorer than the *cis* side ( $\epsilon_c > \epsilon_t$ ). In Fig. 3(c), we present the free energy profile, where the *cis* and *trans* sides have different interaction strengths, i.e.,  $\epsilon_c = -1.0$  and  $\epsilon_t = -0.8$ . While the other features remain the same as in Fig. 3(b), here one observes that the free energy has an upward tilt during the threading stage. This indicates that the polymer prefers to stay inside the channel. Conversely, Fig. 3(d) depicts the reverse situation, where the *trans* side has the lower free energy, indicating that the polymer prefers to stay outside the channel. This indicates that there is a subtle competition between entropy and the internal energy, which modifies the free energy profile. Since the apex angle is constant ( $\alpha = 45^\circ$ ), the entropic contribution arising due to different conformations also remains constant. However, by varying the difference of ( $\epsilon_c - \epsilon_t$ ), one can modify the barrier height.

Another important observation is that when a back wall moves towards the opening of the channel, initially the free energy of the *cis* side remains almost constant, but shows a significant change after  $X = -12.0$ . This is because there is not enough space to accommodate a polymer at the *cis* side and, therefore, there is a significant loss of configurational entropy. Since a flat wall demarcates the *trans* side,

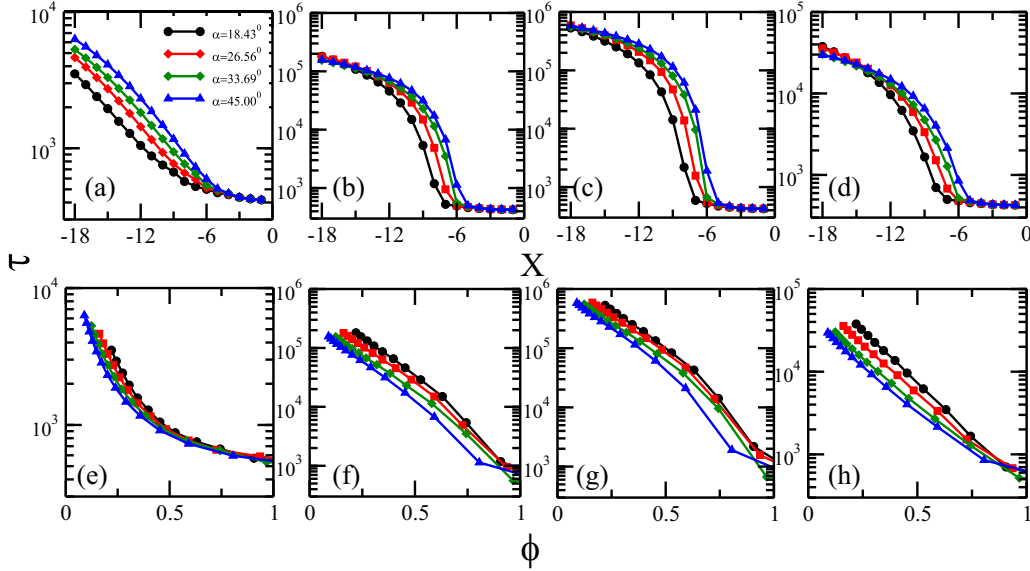


FIG. 4. (a)–(d) The variation of translocation time as a function of the back-wall position  $X$ , and (e),(f) as a function of effective space  $\phi$  for different apex angles  $\alpha$ . The solvent quality is varied on both the *cis* and *trans* sides. (a) and (e) represent the case where there is a good solvent on both sides ( $\epsilon_c = 0.0 = \epsilon_t$ ); (b) and (f) correspond to poor solvent conditions on either side ( $\epsilon_c = -1.0 = \epsilon_t$ ); (c) and (g) depict a situation where the solvent on the *cis* side is poorer compared to the *trans* side  $\epsilon_c = -1.0, \epsilon_t = -0.8$ ; and (d) and (h) present the reverse case where the solvent on the *trans* side is poorer compared to the *cis* side with  $\epsilon_c = -0.8, \epsilon_t = -1.0$ .

the number of conformations remains the same irrespective of the back-wall position. Therefore, the free energy after the translocation of a polymer remains almost the same for all back-wall positions [Figs. 3(a)–3(d)]. When  $X > -6.0$ , the space available to the polymer inside the channel is significantly less; as a result, there is a significant change in the free energy, which is apparent from Figs. 3(a)–3(d). Interestingly, for  $X = -3.0$ , there is not enough space to accommodate even a single conformation, and thus here one can see the contribution of free energy during threading and after the translocation of the entire chain only. It is pertinent to mention here that the qualitative nature of the free energy profile remains the same when we change the apex angle  $\alpha$ .

**C. Translocation dynamics**

The phenomenon of polymer translocation can be well described by considering the average time required for the polymer to move from the initial state (*cis* side) to the final state (*trans* side). This temporal parameter finds applicability in a diverse range of biological processes, e.g., DNA melting, polymer folding, charge hopping, etc. The knowledge of this timescale provides a better understanding of these processes at the cellular level. The diffusion of the chain can be effectively described by the Fokker-Planck equation, enabling the calculation of the time required for the chain to travel from the initial stage, say  $x_0$ , to a specific point  $x_t$ , as expressed by the following equation [34]:

$$\mathcal{T}_{o \rightarrow t} = \frac{1}{D} \int_{x_0}^{x_t} e^{F(x')} dx' \int_{x_0}^{x'} e^{-F(x'')} dx'' \quad (6)$$

The chain diffusivity, denoted as  $D$ , is a variable that exhibits an inverse relationship with the chain length [23]. In line with the approach outlined in Ref. [42], we assign a value

of  $D = 1$ . Given the implementation of a lattice model, Eq. (6) can be represented in a discrete form as

$$\mathcal{T}_{o \rightarrow t} = \sum_{x'=x_0}^{x_t} e^{F(x')} \Delta x' \sum_{x''=x_0}^{x'} e^{-F(x'')} \Delta x'', \quad (7)$$

where  $\Delta x' = \Delta x'' = 1$  because free energy is calculated at an equispaced lattice. The time ( $\tau$ ) required for the polymer to cross the energy barrier imparted by the channel is highly dependent on the nature of the channel geometry and solvent present on either side of the channel. We first consider a good solvent on both sides of the channel ( $\epsilon_c = \epsilon_t = 0$ ), where there is no attractive interaction among monomers. Figures 4(a) and 4(e) show the decay of translocation time ( $\tau$ ) for various angles as a function of back-wall position  $X$  and  $\phi$ , respectively. One can notice that for the apex angle  $\alpha = 45^\circ$ , the value of  $\tau$  is higher compared to  $\alpha = 18.43^\circ$  for the lower values of  $X$  and there is a significant difference in  $\tau$  for different values of  $\alpha$ . Thus, one can infer that confinement promotes the translocation. However, when the back wall is closed to the opening of the channel ( $X > -6.0$ ), the value of  $\tau$  tends to a constant value. It is interesting to note that when we plot the variation of  $\tau$  as a function of  $\phi$ , all the data collapse nearly on a single curve, indicating that for the good solvent, the translocation time  $\tau$  depends only on the fraction of space available to a polymer chain.

If the solvent quality is poor across the channel ( $\epsilon_c = \epsilon_t = -1.0$ ), we find that the translocation time decays up to a certain value of  $X$  and then approaches a constant value [Fig. 4(b)]. In this case, the polymer acquires the conformation of a globule state of relatively smaller size compared to the swollen state. Therefore, if the wall is far away from the opening of the channel, the translocation time remains constant for all apex angles studied here as the polymer does

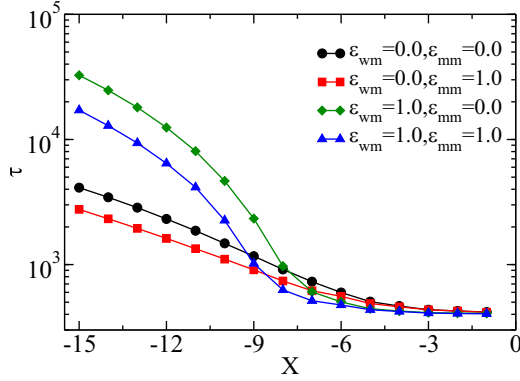


FIG. 5. The variation of translocation time as a function of the back-wall position  $X$ . Four distinct cases are investigated.  $\epsilon_{mm}$  and  $\epsilon_{wm}$  are the interactions among monomers and between monomers and channel walls, respectively.

not see the confinement. As the back wall approaches towards the opening of the channel, we observe a clear difference in  $\tau$ . Like the good solvent case, we also find that confinement advances the translocation; however, the value of  $\tau$  is almost an order higher than the one observed for the good solvent. The increase in the  $\tau$  may be understood from Fig. 3(b), where we observed that the free energy remains constant during threading. Unlike the good solvent, in this case the translocation times are well separated and show a linear decrease with  $\phi$  for all angles. For  $\phi = 1$ , the translocation times for all angles tend to be nearly equal as there is no space in the *cis* side and the *trans* side has equal space for all values of  $\alpha$ .

Interestingly, when the solvent qualities across the channel are different, ( $\epsilon_c = -1.0$   $\epsilon_t = -0.8$ ) and ( $\epsilon_c = -0.8$   $\epsilon_t = -1$ ), we do not see any qualitative change in the translocation behavior except for the value of  $\tau$ . If the *cis* side has a relatively poorer solvent, the free energy during threading has uphill trends and thus hinders the polymer's ability to thread through the opening of the channel, resulting in increased translocation times compared to the similar solvent ( $\epsilon_c = \epsilon_t = -1.0$ ) across the channel. Under reverse solvent conditions ( $\epsilon_c = -0.8$  and  $\epsilon_t = -1.0$ ), the free energy exhibits downhill trends during threading. Consequently, the polymer tends to prefer the *trans* side, leading to a net decrease in  $\tau$ .

#### IV. INFLUENCE OF REPULSIVE FORCES AMONG MONOMERS AND CHANNEL WALL IN POLYMER TRANSLOCATION

We now extend our study where the channel wall is either repulsive or neutral for a polymer. If we consider repulsive interaction in addition to excluded volume in polymer, the model may mimic the case of charged DNA. For this, we choose apex angle  $\alpha = 45^\circ$  and vary the back-wall position. We systematically investigate the intricate dynamics of polymer translocation for four distinct cases, shown in Fig. 5, each offering insights into the specific molecular interactions that play a crucial role in the translocation of charged DNA through confined geometries. First, we show the results where no interactions were considered among monomers, and

between monomers and the channel walls ( $\epsilon_{mm} = 0.0$  and  $\epsilon_{wm} = 0.0$ ), to establish a fundamental baseline scenario of translocation dynamics. This setting provides a crucial reference point against which subsequent cases could be compared. Next, we consider a scenario with no monomer-wall interaction, but included a repulsive force among monomers ( $\epsilon_{wm} = 0.0$  and  $\epsilon_{mm} = 1.0$ ). To our surprise, this configuration resulted in a minimization of translocation time. This may be understood as the repulsive interaction among monomers serves to prevent entanglements (end-to-end distance increases), reducing the likelihood of collisions during the translocation process. In the absence of interactions with the channel walls, monomers experience enhanced freedom of movement, allowing for a smoother and more efficient passage through the cone-shaped channel. This reduced hindrance to motion, facilitated by repulsive forces among monomers, contributes to their efficient navigation within the channel. Moreover, the repulsive interactions foster an optimal exploration of the available space, minimizing unnecessary delays and promoting a streamlined progression through the channel.

Interestingly, in the scenario where the only repulsive interaction existed between the monomer and the channel wall, excluding interactions among monomers ( $\epsilon_{wm} = 1.0$  and  $\epsilon_{mm} = 0.0$ ), we observed an unexpected increase in translocation time compared to the noninteraction scenario. The unexpected delay can be attributed to the influential role of repulsive forces in the cone-shaped channel, which reduces the available space for the polymer. This confinement effect results in a reduction in polymer size due to increased repulsive interaction with the channel walls. Consequently, we observed a delay in translocation time when the monomer-wall interaction was in play, highlighting the significant impact of the repulsive forces in the cone-shaped channel on the translocation dynamics.

The investigation into the combined effects of monomer-monomer and monomer-wall repulsive interactions ( $\epsilon_{mm} = 1.0$  and  $\epsilon_{wm} = 1.0$ ) revealed intriguing dynamics during translocation. When both types of repulsive forces are in play, the polymer encounters a nuanced environment that influences its movement through the cone-shaped channel. The repulsive interaction among monomers prevents excessive clustering, minimizing collisions and entanglements during translocation. Simultaneously, the repulsive force between monomers and the channel wall adds another layer of complexity. The channel, by nature, constrains the available space for the polymer, leading to a reduction in polymer size due to confinement, ultimately affecting the end-to-end distance. This reduction in available space and polymer size contributes to a delayed translocation time compared to scenarios with no interactions among monomers and walls. However, intriguingly, the translocation in this combined scenario is faster than when only the wall exerts a repulsive force. This suggests a delicate interplay between various forces, emphasizing the importance of understanding the nuanced effects of multiple interactions in the translocation process.

These findings not only contribute to our understanding of polymer translocation dynamics through cone-shaped channels, but also offer valuable insights into the specific challenges and optimizations associated with the translocation

of polymer through confined geometries. The unexpected trends observed in certain scenarios open avenues for further exploration and the potential refinement of translocation processes, particularly in the context of charged DNA.

## V. CONCLUSIONS

In this study, we have investigated the influence of confinement on polymer translocation through a cone-shaped channel using the exact-enumeration technique. In contrast to previous investigations, we introduce a finite space on the *cis* side that can be varied, while the *trans* side remains semi-infinite. The space available at the *cis* side can be varied by placing a back wall at different positions away from the opening of the channel. Additionally, the confinement is also varied by changing the apex angle  $\alpha$ , allowing us to observe its effect on polymer translocation. One end of the polymer is anchored on the principal axis, while the other end is free to be anywhere. We systematically vary the position of anchored sites from the *cis* side to the *trans* side, and obtain the exact free energy of the system for a given value of back-wall position  $X$  and the apex angle of the channel  $\alpha$ . Using the Fokker-Planck equation, we obtained translocation times from the free energy of the system having different solvent qualities across the channel.

We place particular emphasis on the contribution made in this work of the calculation of system entropy exactly, which adds to the understanding of the translocation process. Our results, depicted in Fig. 2(a), reveal a clear trend: as the back-wall position  $X$  shifts, the system's entropy decreases. In addition, this effect is amplified when the apex angle  $\alpha$  is reduced. Strikingly, when plotting entropy as a function of  $\phi$  for all  $\alpha$  values, interestingly, all the data points collapse onto a single line. This intriguing finding suggests that up to a certain  $\phi$  threshold, entropy primarily hinges on the space accessible to the polymer within the *cis* side. As the anchored site approaches the opening of the channel, the system's entropy rises, influenced by the portion of the chain that translocates to the *trans* side, boasting semi-infinite space. This intriguing phenomenon ultimately leads to the system's entropy reaching a constant value, irrespective of values of  $\alpha$ .

The translocation time ( $\tau$ ) obtained from the free energy analysis provides valuable insights into the translocation process within a confined environment. In the case of a good solvent,  $\tau$  decreases as the level of confinement increases, either due to the position of the back wall or the confining angle. Remarkably, the most significant finding is that the values of

$\tau$  collapse onto a single curve when plotted against  $\phi$ . This suggests that the translocation time is primarily influenced by the confining space, regardless of its specific shape. Based on this observation, we propose that the inclusion of molecular crowders or similar entities within the channel can potentially expedite the translocation process.

Another interesting finding is that by manipulating the difference in solvent quality across the channel, one can exert control over the translocation process. The linear decrease in  $\tau$  with  $\phi$  for different values of  $\alpha$  indicates the need for further investigation into scaling phenomena. This feature holds potential applications in various fields such as cell metabolism, DNA-RNA sorting and sequencing, and drug delivery mechanisms. These applications involve the transport of biomolecules, which is influenced by the chemical potential gradient of the solvent. We hope that future measurements of translocation times under variable confining environments will contribute to a better understanding of the translocation process.

We also explored polymer translocation through a cone-shaped channel with either repulsive or neutral interactions with the channel wall, mimicking scenarios relevant to charged DNA translocation. Investigating four distinct cases, we uncover intricate dynamics shaping the translocation of charged DNA through confined geometries. The absence of interactions among monomers and channel walls establishes a fundamental baseline, while the introduction of repulsive forces among monomers surprisingly minimizes translocation time, preventing entanglements and enhancing freedom of movement. Unexpected delays arise when only the channel wall exerts a repulsive force, reducing available space and polymer size. Combined monomer-monomer and monomer-wall repulsive interactions introduce nuanced dynamics, emphasizing the intricate interplay between forces and contributing to a delayed but faster translocation compared to scenarios with only wall repulsion. This study provides comprehensive insights into the complex factors influencing polymer translocation through confined channels.

## ACKNOWLEDGMENTS

Financial assistance from the Science and Engineering Research Board, India, UGC, India, Scheme for Promotion of Academic and Research Collaboration scheme of Ministry of Education, and Institution of Eminence scheme, Ministry of Education, India is gratefully acknowledged.

- 
- [1] F. Vella, *Biochem. Educ.* **22**, 164 (1994).
  - [2] S. Nakielny and G. Dreyfuss, *Cell* **99**, 677 (1999).
  - [3] I. J. Molineux and D. Panja, *Nat. Rev. Microbiol.* **11**, 194 (2013).
  - [4] D. Marenduzzo, C. Micheletti, E. Orlandini, and D. W. Summers, *Proc. Natl. Acad. Sci. USA* **110**, 20081 (2013).
  - [5] Z. T. Berendsen, N. Keller, S. Grimes, P. J. Jardine, and D. E. Smith, *Proc. Natl. Acad. Sci. USA* **111**, 8345 (2014).
  - [6] J. Kasianowicz, E. Brandin, D. Branton, and D. Deamer, *Proc. Natl. Acad. Sci. USA* **93**, 13770 (1996).
  - [7] G. F. Schneider, S. W. Kowalczyk, V. E. Calado, G. Pandraud, H. W. Zandbergen, L. M. K. Vandersypen, and C. Dekker, *Nano Lett.* **10**, 3163 (2010).
  - [8] K. Luo, T. Ala-Nissila, S.-C. Ying, and A. Bhattacharya, *Phys. Rev. Lett.* **99**, 148102 (2007).
  - [9] Y.-C. Chen, C. Wang, Y.-L. Zhou, and M.-B. Luo, *J. Chem. Phys.* **130**, 054902 (2009).
  - [10] M.-B. Luo and W.-P. Cao, *Phys. Rev. E* **86**, 031914 (2012).
  - [11] J. M. Polson and D. R. Heckbert, *Phys. Rev. E* **100**, 012504 (2019).

- [12] A. Mohan, A. B. Kolomeisky, and M. Pasquali, *J. Chem. Phys.* **133**, 024902 (2010).
- [13] K. Luo, I. Huopaniemi, T. Ala-Nissila, and S.-C. Ying, *J. Chem. Phys.* **124**, 114704 (2006).
- [14] A. Dabhade, A. Chauhan, and S. Chaudhury, *ChemPhysChem* **24**, e202200666 (2023).
- [15] P.-Y. Hsiao, *ACS Omega* **5**, 19805 (2020).
- [16] K. Luo, S. T. T. Ollila, I. Huopaniemi, T. Ala-Nissila, P. Pomorski, M. Karttunen, S.-C. Ying, and A. Bhattacharya, *Phys. Rev. E* **78**, 050901(R) (2008).
- [17] C. M. Edmonds, Y. C. Hudiono, A. G. Ahmadi, P. J. Hesketh, and S. Nair, *J. Chem. Phys.* **136**, 065105 (2012).
- [18] T. Ikonen, A. Bhattacharya, T. Ala-Nissila, and W. Sung, *J. Chem. Phys.* **137**, 085101 (2012).
- [19] A. Bhattacharya, W. H. Morrison, K. Luo, T. Ala-Nissila, S. C. Ying, A. Milchev, and K. Binder, *Eur. Phys. J. E* **29**, 423 (2009).
- [20] R. H. Abdolvahab, M. R. Ejtehadi, and R. Metzler, *Phys. Rev. E* **83**, 011902 (2011).
- [21] P. M. Suhonen and R. P. Linna, *Phys. Rev. E* **93**, 012406 (2016).
- [22] W. Yu and K. Luo, *J. Am. Chem. Soc.* **133**, 13565 (2011).
- [23] M. Muthukumar, *Phys. Rev. Lett.* **86**, 3188 (2001).
- [24] A. Cacciuto and E. Luijten, *Phys. Rev. Lett.* **96**, 238104 (2006).
- [25] C. T. A. Wong and M. Muthukumar, *Biophys. J.* **95**, 3619 (2008).
- [26] H. Khalilian, J. Sarabadani, and T. Ala-Nissila, *Phys. Rev. Res.* **3**, 013080 (2021).
- [27] F. Tan, Y. Chen, and N. Zhao, *Soft Matter* **17**, 1940 (2021).
- [28] B.-J. Jeon and M. Muthukumar, *Macromolecules* **49**, 9132 (2016).
- [29] N. Nikoofard and H. Fazli, *Phys. Rev. E* **85**, 021804 (2012).
- [30] A. Sharma, R. Kapri, and A. Chaudhuri, *Sci. Rep.* **12**, 19081 (2022).
- [31] W.-J. Lan, D. A. Holden, B. Zhang, and H. S. White, *Anal. Chem.* **83**, 3840 (2011).
- [32] L. T. Sexton, L. P. Horne, and C. R. Martin, *Mol. BioSyst.* **3**, 667 (2007).
- [33] Z. Siwy and A. Fuliński, *Phys. Rev. Lett.* **89**, 198103 (2002).
- [34] W. Sung and P. J. Park, *Phys. Rev. Lett.* **77**, 783 (1996).
- [35] M. Muthukumar, *J. Chem. Phys.* **111**, 10371 (1999).
- [36] M. Muthukumar, *J. Chem. Phys.* **118**, 5174 (2003).
- [37] A. J. Guttmann and G. M. Torrie, *J. Phys. A: Math. Gen.* **17**, 3539 (1984).
- [38] S. Kumar, K. Chauhan, S. Singh, and D. Foster, *Phys. Rev. E* **101**, 030502(R) (2020).
- [39] K. Chauhan and S. Kumar, *Phys. Rev. E* **103**, 042501 (2021).
- [40] C. Vanderzande, *Lattice Models of Polymers* (Cambridge University Press, Cambridge, 1998).
- [41] S. Kumar and M. S. Li, *Phys. Rep.* **486**, 1 (2010).
- [42] L.-Z. Sun, W.-P. Cao, and M.-B. Luo, *J. Chem. Phys.* **131**, 194904 (2009).